Akademie věd České republiky
Ústav teorie informace a automatizace, v.v.i.

Academy of Sciences of the Czech Republic
Institute of Information Theory and Automation

RESEARCH REPORT

P. Pecha, O. Tichý, E. Pechová

Potential Radioactive Hot Spots Induced by Radiation Accident Being Underway of Atypical Low Wind Meteorological Episodes

No. 2382 April 29, 2020

ÚTIA AV ČR, P. O. Box 18, 182 00 Prague, Czech Republic
Tel: (+420) 266052009, Fax: (+420) 286890378, Url: http: //www.utia.cas.cz,
Email: utia@utia.cas.cz

This report constitutes an refereed manuscript, which is intended to be submitted for publication. Any opinions and conclusions expressed in this report are those of the authors and do not necessarily represent the views of the Institute.

Obsah

Abstract

A special method has been developed for estimation of a certain hypothetical radioactivity release with potentially high variability of the source strength. The interactions of the radioactive cloud with surface and atmospheric precipitation are examined and possible adverse consequences on the environment are estimated. The worst-case scenario is devised in two stages starting with a calm meteorological situation succeeded by wind. At the first stage, the discharges of radionuclides into the motionless ambient atmosphere are assumed. During several hours of this calm meteorological situation, a relatively significant level of radioactivity can be accumulated around the source. At the second stage, the calm is assumed to terminate and convective movement of the air immediately starts. The pack of accumulated radioactivity in the form of multiple Gaussian puffs is drifted by wind and pollution is disseminated over the terrain. The results demonstrate the significant transport of radioactivity even behind the protective zone of a nuclear facility (up to between 15 and 20 km). In the case of rain, the aerosols are heavily washed out and dangerous hot spots of the deposited radioactivity can surprisingly emerge even far from the original source of the pollution.

1 Introduction

Hazardous effects of a potential accidental radioactive release during an atypical episode of the low wind speed condition are examined. A realistic experiment is carried out, when a radioactivity is accidentally released into the calm atmospheric conditions (motionless atmospheric environment). During several hours of the calm situation, the dangerous radioactivity values can be locally accumulated. Afterwards, the calm is assumed to be immediately succeeded by the windy convective transport and the harmful substances are successively disseminated in the surrounding environment. Notably, during combination with potential occurrence of the atmospheric precipitation, the hot spots with significantly increased radioactivity deposited on the ground were determined.

Long-term meteorological records in the territory of the Czech Republic assess the probability of occurrence of low-wind (< 0.5 $m.s^{-1}$) meteorological episodes in a wide range from several percents up to about 14 %. The duration of the situation fluctuates between tens of minutes to several hours. We have analysed long-term series of the archived hourly meteorological data forecasted for the points of the nuclear power plant (NPP) localities provided by the Czech hydro-meteorological service. A specific pre-processing of the archived data was carried out for purposes of this article. The sequences denoted as SEQ^* with at least three uninterrupted consecutive data records with low-wind speed < 0.5 $m.s^{-1}$ have been collected (it means, continuous low wind speed intervals ≥ 3 hours). The results in Table 1 for locations of the NPP Dukovany (EDU) and NPP Temelin (ETE) indicate a wide variability for different localities and time periods.

Table 1: Selection of low wind speed (< 0.5 $m.s^{-1}$) continuous sequences SEQ^* with duration ≥ 3 hours.

NPP (year)	$N(SEQ^*)$ number of SEQ^*	$P(SEQ^*)$ percentage of SEQ^*	$L(SEQ^*)_{max}$ longest SEQ^* (hours)
EDU (2018)	28	1.574	12
EDU (2017)	51	2.789	10
EDU (2016)	58	3.052	10
EDU (2015)	50	2.675	14
EDU (2014)	51	4.122	11
ETE (2018)	79	4.529	15
ETE (2017)	76	4.305	20
ETE (2016)	98	5.292	11
ETE (2015)	100	5.406	14
ETE (2014)	126	8.266	18
ETE (2008 -2009) [(1)]	230	8.737	35

[(1)] 17 520 hourly records

Although the probability of a long low wind speed episode is low, possible radiological impact on the surrounding environment can be serious. The problem of low wind speed can be theoretically treated as a continuous release described traditionally in representation of the

Gaussian dispersion model. It was generally believed that commonly used steady-state Gaussian dispersion models such as AERMOD (EPA, 2004) or ADMS (*Carruthers et al.* , 2003) are not applicable to situations when the wind speed close to the ground are comparable to the standard deviation of the horizontal velocity fluctuation. The performance of the Gaussian dispersion models was poor and concentration values during the case of the low wind speed episodes were highly overpredicted. Very little model evaluations for these low wind conditions have been revealed. Formerly, some approximations were proposed for solution of the calm problem. The idea intended in the European environmental code RODOS (Real time Online DecisiOn System) assumed the equivalent plume segment to return many-times alternately over the source. (Demonstration also in *Pecha and Pechova, (2004)*).

Thanks to initiative of US Environmental Protection Agency (EPA), the model formulation changes and subsequent new model evaluation have been performed. After many years of testing and review, the refinements have been implemented and performance of two steady-state models under low wind speed conditions was examined in *Qian and Venkatram, (2011).* For AERMOD Model Version 123455 (*Jeffrey et al., 2013)*, the most important new option addresses the former overpredicted concentration estimates. The option increases minimum horizontal turbulence and incorporate a modified meander component. An interesting result has brought the comparison with application of Lagrangian dispersion model (*Rakesh et al., 2019)* for the case of the low wind speed conditions. The performance of the Gaussian model with improved dispersion parameters and a specific Lagrangian dispersion model is in good agreement. Profound overview of the significant references and methodology improvements are given in *Pandey and Sharan (2019).* The segmented plume approach with all new options is recommended here as reasonably well for modelling of dispersion of a pollutant in low wind speed conditions. The effect of low wind conditions and wind intervals in low wind speed are treated in *Hyojoon et al.,(2013*). The influence of definition of the calm conditions and classification of the low wind speed intervals on atmospheric dispersion factors using a Gaussian plume model is documented.

This paper introduces a simplified scenario of the real calm situation when radioactive pollution is discharged into the motionless surroundings. Generally used algorithms for Gaussian puff model (e.g. *Adriaensen, 2002)* seem to be suitable for these purposes. Development of the puff model for a sequence of discrete discharges is described in this paper. In this way, also the potential strong changes of the release dynamics of the harmful substances can be simulated by long sequences of different short-term instantaneous puffs. The important question related to the strict definition $u=0\ m.s^{-1}$ for the calm situation is illustrated in the following example. The real sequence of eight hourly meteorological inputs in Table 2 (shaded) shows very low wind speeds having more or less chaotic fluctuations. Moreover, the trajectory constructed from this eight points *(wind speed, wind direction)* is restricted to very close region. We assume the situations to be well approximated by the calm situation ($u \rightarrow 0\ m{\cdot}s^{-1}$) with duration of eight hours. Rising wind in the ninth hour breaks up the calm situation.

Table 2. A sequence of hourly meteorological data which could be considered as a calm (grey region), provided from archive of the Czech hydro-meteorological service for coordinates of the NPP Dukovany, started at Oct. 25, 2015, 03.00 CET.

Time_stamp	Pasquill_cat.	wind_speed	wind_dir.	rain
yyyymmddhh	-	at 10m height $m{\cdot}s^{-1}$	$(°)^{(*)}$	$mm.hour^{-1}$
......	......	......	......	......
2015102423	C	0.7	138	0
2015102500	D	0.8	52	0

2015102501	D	0.5	18	0
2015102502	D	0.5	26	0
2015102503	D	0.4	298	0
2015102504	F	0.3	304	0
2015102505	F	0.2	85	0
2015102506	F	0.2	170	0
2015102507	F	0.2	172	0
2015102508	C	0.3	229	0
2015102509	B	0.2	110	0
2015102510	B	0.2	339	0
2015102511	B	1.9	324	0
2015102512	C	2.1	341	0
2015102513	C	3.3	0	1.0
2015102514	D	3.3	333	1.0
......	......	......	......	......

(*) clockwise, from North

2 The First Stage: An Approximation Based on Series of Consecutive Discrete Puffs Released into the Stationary (Motionless) Ambience

Radiological consequences of the release of radionuclides during the calm conditions are treated as a superposition of an equivalent chain of Gaussian puffs from the elevated source. Each puff has its own nuclide inventory and strength of released activity. The whole release is assumed to proceed under zero horizontal wind speed and each puff has a shape of a gradually-spreading discus with its centre at the source of the pollution. The radioactivity concentration in the air is described by the Gaussian-puff distribution where the vertical and horizontal dispersion coefficients are expressed by time-dependent empirical recommendations based on the field measurements under low-wind speed conditions (*Okamoto et al.*, 1999). Similarly, the calm wind dispersion parameters for the puff model in the RASCAL code (*McGuire et al., 2007*) are switched from distance-based to time-based entities. Each puff is modelled at all consecutive time stages, taking into account the depletion of activity due to the removal mechanisms of radioactive decay, dry activity deposition on the ground, and washout caused by the atmospheric precipitation. The dry deposition during calm is roughly estimated when only a certain fraction corresponding to the gravitational settling is considered.

The total number *M* of discrete pulses of radionuclide *n* are released from an elevated point source at a height *H (x=0; y=0; z=H)* inside the mixing layer during the calm episode in the time interval $\left\langle T_{START}^{CALM}; T_{END}^{CALM} \right\rangle$. The first pulse starts in the beginning of the accident *T**. A chain of the corresponding discrete releases Q^n_m , *m=1, ... , M* are ejected step by step with the consecutive time periods Δt_m . This situation is demonstrated in Figure 1 where the release dynamics for one particular discharge Q^n_m (belonging to puff *m*) from the chain is shown. The originality of the scheme in Figure 1 consists in the fact that various parameter changes among the pulses *m* inside the calm region can be taken into account (release source strength, isotopic composition, atmospheric stability class, rainfall, possibly height of release *H*). Capability to model continuous release using a large number of discrete pulses *m* is evident.

Let the m^{-th} puff be born at the starting point of the interval Δt_m, that is, at time $t_m = \sum_{k'=1}^{k=m-1} \Delta t_k$ after the beginning of the accident. The pulse of discharge Q^n_m (in Bq) of radionuclide *n* just at the starting point of the interval Δt_m can be different for each adjacent interval. As stated above, it relates to the period of duration, specific group of leaking radionuclides with specific source strength, occurrence of atmospheric precipitation, etc. The source strength from the elevated source at a height *H (x=0; y=0; z=H)* for the time period Δt_m is denoted by $S_m^n(t)$ (in Bq/s). For discrete puff, we use a symbolic notation

$$Q_m^n = \int_{(\Delta t_m)} S_m^n(t) \cdot dt \tag{2.1}$$

Where, for the instantaneous puff, the source strength can be expressed with the assistance of delta function around t_m.

We shall focus on diffusion of one particular puff *m* in its further stages up to the moment T_{END}^{CALM}. It propagates within consecutive time intervals *i*, (*i= 1, ... , M-m+1*) relative to *m*. The "age" of the original puff *m* at the end of its successive relative interval *i* is denoted as $t_{m,i} = \sum_{k=1}^{k=i} \Delta t_{m,k}$. The layout is drawn in Figure 1.

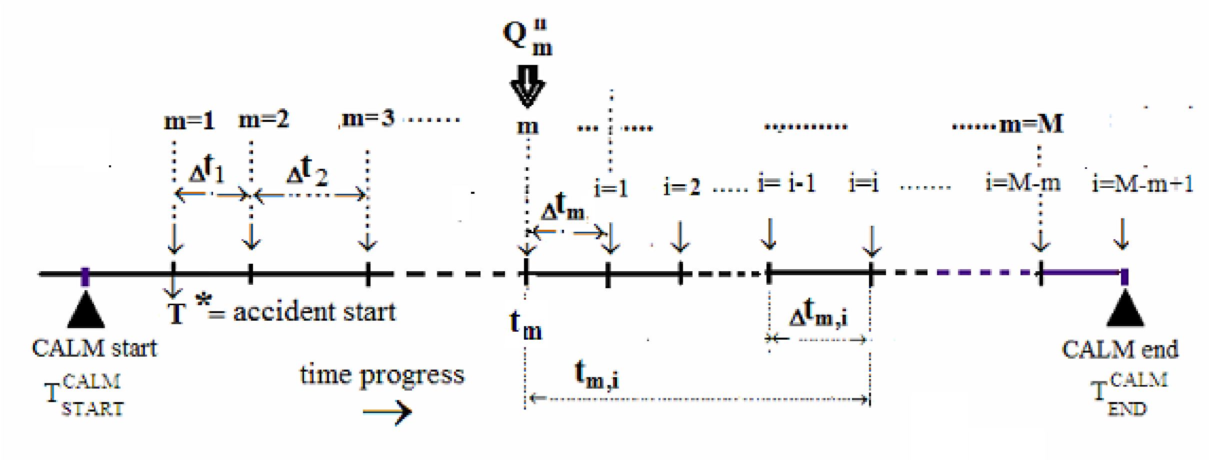

Figure 1: The original detailed scheme of the time progress of the discrete radioactivity discharges into the motionless ambience during the calm meteorological episode.

The activity concentration $C_{m,i}^n$ [Bq/m^3] of radionuclide *n* in the air for the puff born in the interval *m* with the original discharge $Q^n{}_m$ which reaches the end of the time interval *i at* $t_{m,i}$, is described by the modified 3-D Gaussian puff formula (e.g., *Zannetti*, 1990; *Carruthers et al.*, 2003) as :

$$C_{m,i}^n\left(t_{m,i}\,;x,y,z\right) = \frac{Q_m^n}{(2\pi)^{3/2}\cdot\sigma_x\left(t_{mi,}\right)\cdot\sigma_y\left(t_{m,i}\right)}\cdot\exp\left[-\frac{1}{2}\left(\frac{x^2}{\sigma_x{}^2\left(t_{m,i}\right)}+\frac{y^2}{\sigma_y{}^2\left(t_{m,i}\right)}\right)\right]\times$$

$$\times\left\{\Psi\left(z,\sigma_z\left(t_{m,i}\right),h_{ef,m}\right)+\Re_{refl}^n\right\}\times f_R^n(t_m\to t_{m,i})\cdot f_F^n(t_m\to t_{m,i})\cdot f_W^n(t_m\to t_{m,i}) \tag{2.2}$$

$$\text{where}\quad \Psi\left(z,\sigma_z\left(t_{m,i}\right),h_{ef,m}\right)=\frac{1}{\sigma_z\left(t_{m,i}\right)}\cdot\left\{\exp\left(-\frac{\left(z-h_{ef,m}\right)^2}{2\cdot\sigma_z^2\left(t_{m,i}\right)}\right)+\exp\left(-\frac{\left(z+h_{ef,m}\right)^2}{2\cdot\sigma_z^2\left(t_{m,i}\right)}\right)\right\}$$

It stands for stable conditions, providing there is no inversion. The puff is assumed to continue growing in time (during the calm situation) or growing downstream in the convective transport, relatively to its centre. The function Ψ in compound bracket stands successively for the growth of actual puff and its reflection in the ground plane. The additional multiple reflections $\mathfrak{R}^{n}_{refl}$ on the ground and the inversion layer/mixing height for this near-field model are ignored. The factors *f* pertain to the radioactivity depletion from the cloud (see below).

For further calculation the expression (2.2) should be somewhat rewritten. We assume the puff shape to be symmetrical in the *x* and *y* directions. Hence, *x* and *y* can be replaced by the horizontal distance *r* from the centre of the puff. Let us assume that the puff Q^{n}_{m} of radionuclide *n* born at interval *m* propagates and reaches the subsequent time intervals *i*. The stepwise procedure used here means that for each interval *i* the puff "stays on" here for the time period $\Delta t_{m,I}$. The symbol $C_{m,i}$ from Eq. (2.2) above stands for the radioactivity concentration at the end of the interval Δt_{mi}, denoted by $t_{m,i}$. Furthermore, when introducing the relative time *t* inside the interval $\Delta t_{m,i}$, $t \in <0, \Delta t_{m,,i}>$, the modified equation (2.2) for the concentration shape within the interval $\Delta t_{m,i}$ can be expressed (provided that $\sigma_x = \sigma_y = \sigma_r$, $x^2+y^2 = r^2$; only one reflection from ground level is accepted) in the form:

$$C^{n}_{m,i}(t; r, z) = \frac{Q^{n}_{m,i}(t)}{(2\pi)^{3/2} \cdot \sigma^{2}_{r}(\tilde{t}_{m,i})} \cdot \exp\left(-\frac{r^2}{2 \cdot \sigma^{2}_{r}(\tilde{t}_{m,i})}\right) \times \Psi\left(z, \sigma_z(t_{m,i}), h_{ef,m}\right) \qquad (2.2a)$$

Analogically, the near-ground activity concentration in the air equals

$$C^{n}_{m,i}(t; r, z=0) = \frac{2 \cdot Q^{n}_{m,i}(t)}{(2\pi)^{3/2} \cdot \sigma^{2}_{r}(\tilde{t}_{m,i}) \cdot \sigma_z(\tilde{t}_{m,i})} \cdot \exp\left(-\frac{r^2}{2 \cdot \sigma^{2}_{r}(\tilde{t}_{m,i})}\right) \cdot \exp\left(-\frac{(h_{ef,m})^2}{2 \cdot \sigma^{2}_{z}(\tilde{t}_{m,i})}\right) \qquad (2.2b)$$

where $$Q^{n}_{m,i}(t) = Q^{n}_{m} \cdot f^{n}_{R}(t_m \rightarrow \tilde{t}_{m,i}) \cdot f^{n}_{F}(t_m \rightarrow \tilde{t}_{m,i}) \cdot f^{n}_{W}(t_m \rightarrow \tilde{t}_{m,i}) \qquad (2.3)$$

$$\tilde{t}_{m,i} = t_{m,i-1} + t \ ; \ t \in <0, \Delta t_{m,,i}>$$

Equations (2.2), (2.2a) and (2.2b) represent a modification of an expression commonly used in the so-called “source depletion” approach, in which the factors f_R, f_F and f_W represent the depletion of the radionuclide concentration in the puff due to radioactive decay, dry activity deposition and washout of activity induced by possible atmospheric precipitation. The radioactive decay and washout by precipitation are accomplished throughout the entire puff volume. The dry deposition is predominantly driven by the interactions of the surface structures with the ground-level air in the puff. The source depletion model introduces the depletion factors of the original total radioactivity discharge, which accounts for the depletion during the time evolution from $t_m \rightarrow t_{m,i}$. A more detailed comparison of the "source depletion" and an alternative "surface depletion" approach can be found, e.g. in *Horst W. T., 1977.*

2.1 Depletion of stationary puff due to radioactive decay

The radioactive decay is accomplished throughout the entire puff volume, and the corresponding depletion between $<t_0; t>$ generally proceeds proportionally to $exp[-\lambda \cdot (t-t_0)]$. Specifically, the depletion of the original puff *m* up to its relative interval *i* is driven according to

$$f_R^n(t_{m,i}) = \prod_{k=1}^{k=i} \exp(-\lambda^n \cdot \Delta t_{m,k}) = \exp(-\lambda^n \cdot t_{m,i}) \tag{2.4}$$

where λ^n [s^{-1}] denotes the constant of the radioactive decay.

2.2 Depletion of stationary puff due to dry deposition (FALLOUT)

The puff activity concentration depletion due to the dry deposition results from both the gravitational settling and the interaction within the surface layer. The smaller aerosol particles (0.1 to 1 μm) survive for a long time in the plume, and their depletion from the plume is mainly caused by interaction with the surface structures (depending on roughness and friction velocity). In general, the values of the gravitational settling speed vary, depending on the atmospheric stability, wind speed and surface conditions. For calm conditions, we shall restrict our consideration to a simplified recommendation, related only to the process of gravitational settling for the aerosol particles. The properties of the particles have an important role in the radiological hazard. The process is significant for particles with higher diameter values, which do not remain airborne for a long time A brief summary of gravitational settling is described in *Hanna (1982)* or *Pollanen et al., (1995).* Sedimentation velocity as a function of particle aerodynamic diameter, particle shape, particle composition, surface characteristics, charge or possible coagulation processes is in-depth studied in *Tsuda et al., (2013)*. Roughly estimated value vg^n_{grav} = 0.008 m·s^{-1} is used here. It could be accepted for aerosol particles with radii about 5-10 μm. A comment on small aerosol particles (~ 1μm) is mentioned in Section 5.

Let as assume the relative time variable t from the interval $\Delta t_{m,i}$, $t \in <0, \Delta t_{m,i}>$. We search for the total activity in the puff $Q_m^n(t_{m,i-1}+t)$ within the interval $\Delta t_{m,i}$ corresponding to $Q_m^n(t_{m,i-1}+t) \in \langle Q_m^n(t_{m,i-1}), Q_{m,i}^n(t_{m,i}) \rangle$. The near-ground activity concentration $C_{m,i}^n(t; r, z=0)$ in the interval $t \in <0, \Delta t_{m,i}>$ is gradually depleted according to Eq. (2.2b). The total dry deposition flux on the ground $\dot{\Omega}_{m,i}^n(t; z=0)$ [Bq.s^{-1}] from the whole puff (m,i), just at its position at time t, is given by

$$\dot{\Omega}_{m,i}^n(t; z=0) = \int_0^\infty vg_{grav}^n \cdot C_{m,i}^n(t; r, z=0) \cdot 2\pi \cdot r \cdot dr \tag{2.5}$$

The near-ground activity concentration $C_{m,i}^n(t; r, z=0)$ from Eq. (2.2b) is substituted here and, after integration, the resulting total flux of activity of radionuclide n deposited on the ground [Bq·s^{-1}] due to fallout equals

$$\dot{\Omega}_{m,i}^n(t; z=0) = Q_{m,i}^n(t) \cdot \sqrt{\frac{2}{\pi}} \cdot vg_{grav}^n \frac{1}{\sigma_z(t_{m,i-1}+t)} \cdot \exp\left(-\frac{h_{ef}^2}{\sigma_z{}^2(t_{m,i-1}+t)}\right)$$

The source strength reduction inside the interval $\Delta t_{m,i}$ due to the deposits on the ground is expressed as $dQ_{m,i}^n(t)/dt = -\dot{\Omega}_{m,i}^n(t; z=0)$, and finally we have

$$\frac{dQ_{m,i}^n(t)}{Q_{m,i}^n(t)} = -\sqrt{\frac{2}{\pi}} \cdot vg_{grav}^n \frac{1}{\sigma_z(t_{m,i-1}+t)} \cdot \exp\left(-\frac{h_{ef}^2}{\sigma_z{}^2(t_{m,i-1}+t)}\right) \cdot dt \tag{2.6}$$

It results in stepwise source depletion due to the activity deposits on the ground according to

$$Q^n_{m,i} = Q^n_{m,i-1} \cdot \exp\left\{ -\sqrt{\frac{2}{\pi}} \cdot vg^n_{grav} \int_{t=0}^{t=\Delta tmi} \left[\frac{1}{\sigma_z\left(t_{m,i-1}+t\right)} \cdot \exp\left(-\frac{h^2_{ef}}{\sigma_z{}^2\left(t_{m,i-1}+t\right)} \right) \right] dt \right\} \qquad (2.7)$$

<u>*Comment on notation in further text*</u>*:* $Q^n_{m,i}$ *belongs to the value at* $t_{m,i}$*, thus* $Q^n_{m,i} = Q^n_{m,i}\left(t = t_{m,i}\right)$

Let us consider the chain:

$Q^n_{m,i} \,/\, Q^n_m = \left(Q^n_{m,i} \,/\, Q^n_{m,i-1}\right)\cdot\left(Q^n_{m,i-1} \,/\, Q^n_{m,i-2}\right)\cdot \ldots\ldots\ldots \cdot\left(Q^n_{m,i=2} \,/\, Q^n_{m,i=1}\right)\cdot\left(Q^n_{m,i=1} \,/\, Q^n_m\right)$

The final form for dry (FALLOUT) deposit depletion factor $f^n_F\left(t_{m,i}\right)$ for *i-th* time interval relative to the real original discharge Q^n_m leaked out at interval *m* is:

$$f^n_F\left(t_{m,i}\right) = Q^n_{m,i} \,/\, Q^n_m = \prod_{\mathbf{k}=1}^{k=i} \exp\left\{ -\sqrt{\frac{2}{\pi}} \cdot vg^n_{grav} \int_{(t_{mk})} \left[\frac{1}{\sigma_z\left(t_{m,k}\right)} \cdot \exp\left(-\frac{h^2_{ef}}{\sigma_z{}^2\left(t_{m,k}\right)} \right) \right] dt_{m,k} \right\} \qquad (2.8)$$

The total dry deposition on the ground from the puff (*m,i*) is expressed as $\Omega^n_{m,i} = \dot{\Omega}^n_{m,i}(z=0) \cdot \Delta t_{m,i}$.

2.3 Wet deposition (WASHOUT) from stationary puff

Radioactivity concentration $C^n_{m,i}\left(t; r, z\right)$ of nuclide *n* in the puff (originally born at moment t_m) during its next stage *i* is expressed by Eq. (2.2a). We assume the rain at a constant precipitation rate $\upsilon_{m,i}$ [mm·h^{-1}] during the entire interval $\Delta t_{m,i}$. The deposition activity rate of nuclide *n* being washed out from the cloud is expressed using washing coefficient $\Lambda_{m,i}{}^n = a \cdot \upsilon_{m,i}{}^b$ [s^{-1}]. Constants *a* and *b* depend on the physical-chemical form of the radionuclide *n* (different for aerosol, elemental, organic form, zero for noble gases).

Let us assume again the relative time variable *t* from interval $\Delta t_{m,i}$, $t \in < 0 , \Delta t_{m,i} >$. We search for the total activity in the puff $Q^n_{m,i}\left(t\right)$ within the interval $\Delta t_{m,i}$ corresponding to $Q^n_{m,i}\left(t\right) \in \langle Q^n_{m,i-1}, Q^n_{m,i} \rangle$. The activity concentration $C^n_{m,i}\left(t\,; r, z\right)$ in the interval $t \in < 0 , \Delta t_{m,i} >$ is gradually depleted according to Eq. (2.2a). The total wet deposition flux $\dot{W}^n_{m,i}$ [Bq.s^{-1}] from the puff (*m,i*) (puff *m* in its successive time interval *i*) just at its position inside in the time *t* is given by

$$\dot{W}^n_{m,i}\left(t\right) = \int_0^\infty \left[\Lambda^n_{m,i} \cdot \int_0^\infty C_{m,i}\left(t; r, z\right) \cdot dz \right] \cdot 2\pi \cdot r \cdot dr \qquad (2.9)$$

After integration, the resulting flux of activity of radionuclide *n* [Bq·s^{-1}] deposited on the ground due to the washout is

$$\dot{W}^n_{m,i}\left(t\right) = \sqrt{\frac{2}{\pi}} \cdot \Lambda^n_{m,i} \cdot Q^n_{m,i}\left(t\right) \cdot \int_0^\infty \Psi\left(z, \sigma_z\left(t_{m,i-1}+t\right), h_{ef,m}\right) \cdot dz \qquad (2.10)$$

The source strength reduction on interval (m,i) due to the wet deposition on the ground is expressed as $dQ^n_{m,i} \big/ dt = -\dot{W}^n_{m,i}$ and, using expression (2.10), we get

$$\left.\frac{dQ^n_{m,i}(t)}{Q^n_{m,i}(t)}\right|_{wash} = -\Lambda^n_{m,i}\cdot\sqrt{\frac{2}{\pi}}\cdot\left\{\int_0^\infty \Psi\left(z,\sigma_z\left(t_{m,i-1}+t\right),h_{ef,m}\right)\cdot dz\right\}\cdot dt \tag{2.11}$$

It results in a stepwise source depletion due to the washout in interval $\Delta t_{m,i}$ according to

$$\left(Q^n_{m,i}/Q^n_{m,i-1}\right) = \exp\left\{-\sqrt{\frac{2}{\pi}}\cdot\Lambda^n_{m,i}\cdot\int_{(t=0)}^{t=\Delta tm,i}\left[\int_0^\infty \Psi\left(z,\sigma_z\left(t_{m,i-1}+t\right),h_{ef,m}\right)\cdot dz\right]dt\right\} \tag{2.12}$$

Let us consider the chain:

$$\left.(Q^n_{m,i}/Q^n_m)\right|_{wash} = \left(Q^n_{m,i}/Q^n_{m,i-1}\right)_{wash}\cdot\left(Q^n_{m,i-1}/Q^n_{m,i-2}\right)_{wash}\cdot\ldots\cdot\left(Q^n_{m,2}/Q^n_{m,1}\right)_{wash}\cdot\left(Q^n_{m,1}/Q^n_m\right)_{wash}$$

The integral washing factor in the entire interval <$t_m \rightarrow t_{m,i}$> is then marked as:

$$f^n_W\left(t_{m\rightarrow m,i}\right) = Q^n_{m,i}/Q^n_m = \tag{2.13}$$

$$= \prod_{\mathbf{k}=1}^{k=i}\exp\left\{-\sqrt{\frac{2}{\pi}}\cdot\Lambda^n_{m,k}\cdot\int_{(t=0)}^{t=\Delta tm,k}\left[\int_0^\infty \Psi\left(z,\sigma_z\left(t_{m,k-1}+t\right),h_{ef,m}\right)\cdot dz\right]dt\right\}$$

For $k=1$ is used $t_{m,k-1} = t_m$.

We should keep in mind that $\Lambda^n_{m,k}$ depends locally on average precipitation v_k in interval $\Delta t_{m,k}$. Finally, with an assumption of a constant intensity of the rain within the interval $\Delta t_{m,}$, the total activity $W^n_{m,i}$ washed out on the ground is expressed as

$$W^n_{m,i} = \int_{(t=0)}^{t=\Delta tm,k}\dot{W}^n_{m,i}\,dt$$

<u>*Comment*</u>: Even if the rain occurs only in the interval *i*, it also impacts all of the previous puffs *i=1, ... , i-1* contained in the bunch of the Gaussian mixture in the stationary calm region.

3 Evaluation of Radiological Quantities Just at the Moment T^{CALM}_{END} of the Calm Episode Termination

The radioactivity accumulated in the stationary ambient atmosphere is given by superposition of results of all partial pulses *m* in their final phases just when reaching the end of the calm period. The total overall radioactivity concentration in the stationary package of air at the moment of the calm termination can schematically be expressed in agreement with the sketch shown in Figure 1 as

$$C^n\left(T^{CALM}_{END};r,z\right)^{TOTAL} = \sum_{m=1}^{m=M} C^n_{m,i=M-m+1}(r,z) \tag{3.1}$$

where $C^n_{m,i=M-m+1}(r,z)$ is constructed according to scheme in Figure 1.

The total package of radioactivity just at calm end T^{CALM}_{END} consists of superposition of multiple Gaussian puffs *m*, each with the concentration value $C^n_{m,i=M-m+1}$. It belongs to the original partial discharge of radioactivity Q^n_m, which dissipates into the motionless ambient just up to the calm termination. As stated above, the first stage of the scenario after the calm terminates is immediately succeeded by the second stage of the convective movement in the atmosphere. The wind is assumed to start blowing, which immediately drifts and scatters the original stationary heap of the radioactivity over the terrain. The results of the calm situation just at the moment T_{END}^{CALM} are shown in Figure 2. It represents the initial conditions for description of the subsequent convective transport. One of the following two alternative procedures could provide a reasonable solution:

a) The movement within each individual Gaussian puff m with activity concentration $C_{m,i=M-m+1}^{n}$ from (3.1) is separately treated in all of its successive convective stages. The resulting radiological quantities are then given by the superposition for all puffs m.

b) The algorithm developed here for convective transport is based on Gaussian puffs. But superposition of all partial puffs M is evidently non-Gaussian (bottom in Figure 2). An attempt is made when estimating the statistical properties of $C^{n}\left(T_{END}^{CALM};r,z\right)^{TOTAL}$ in advance and examine a possibility to substitute the Gaussian mixture drifted by wind with one representative equivalent Gaussian "superpuff" (personal communication - interview with dr. Miroslav Kárný, Inst. of information theory, Prague, March 2019). The benefit in reduction of the computational load should be evident, mainly for a large number M (simulation of the continuous release).

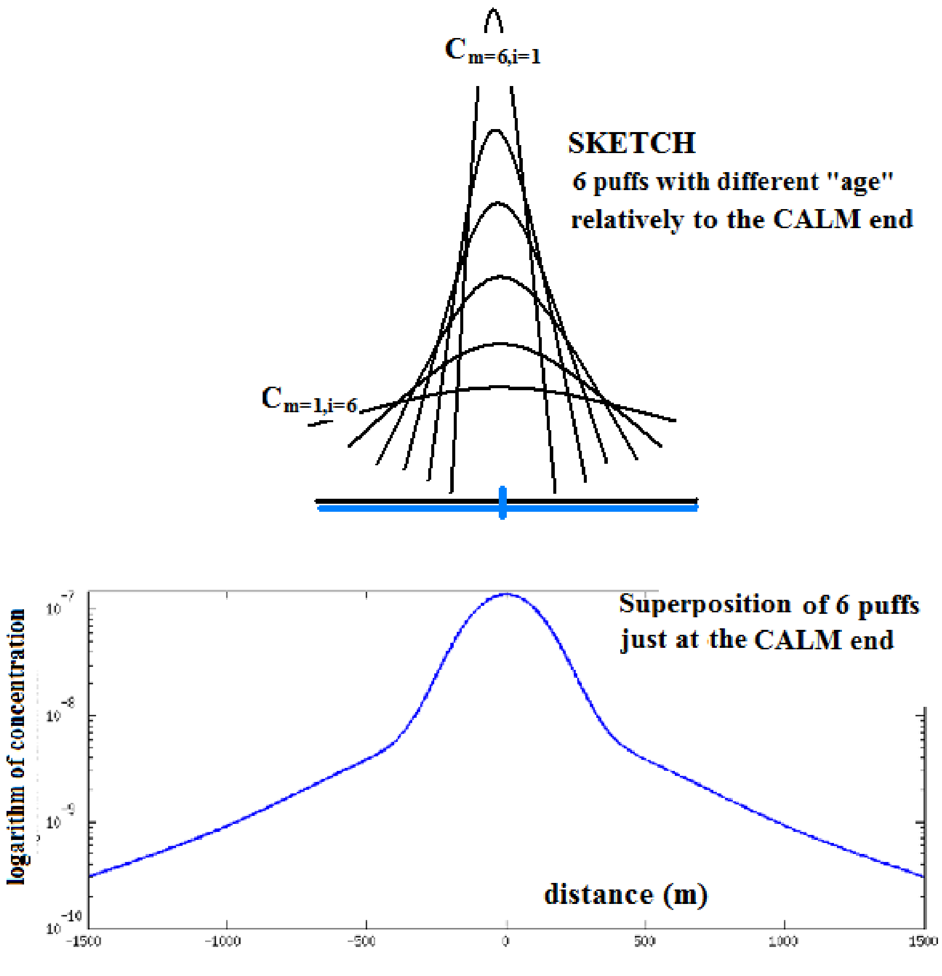

Figure 2: Composition of the resulting distribution (bottom) from the individual discrete puffs (on top).

4 The Second Stage: Previous Stationary Heap of Radioactivity is Immediately Drifted according to Changes of Meteorological Conditions

An elementary basic formulation for small-scale advection of puffs under stable and neutral conditions is adopted. The puffs are assumed to be symmetrical in the *x* and *y* directions and can be replaced by the horizontal distance *r*. The centre of the puff is linearly moving in the direction of the wind. The relative diffusion with regard to the puff centre is in progress. Hourly changes in the meteorological situation are available and the segmented Gaussian puff model is used. Within each hour, the propagation is straightforward and changes are coming up all at once for the given hour. This paper focuses on the near-field analysis in a smaller domain and below the mixing layer. We do not consider more sophisticated but computationally expensive modelling that would account for puff meandering or puff furcation. The puff model with these limitations has been included in the bunch of the dispersion models of the HARP system (HARP, *2010-2019)*.

We shall follow the procedure a) from Section 3. The individual discharge $Q^n{}_m$ is gradually spreading inside the original calm region in such a way that the corresponding partial radioactivity concentration in the air just at the moment T_{END}^{CALM} is denoted by $C_{m,i=M-m+1}^{n}$, or $C_m^n\left(r, z; T_{END}^{CALM}\right)$. The original position of the previous calm region centre was (*x=0; y=0; z=H*). The convective movement in the direction of $\vec{u}_1$ starts from there at T_{END}^{CALM}. Movement of the puff at each stage *p* is assumed to be composed from the absolute overall straight-line translations with velocity values $\vec{u}_p$ and relative dispersions around the puff centre with the dispersion parameters dependent on the translation shifts. Available hourly meteorological data enables to account, step by step, for the relevant scenario parameter changes (see the chart in Fig. 3).

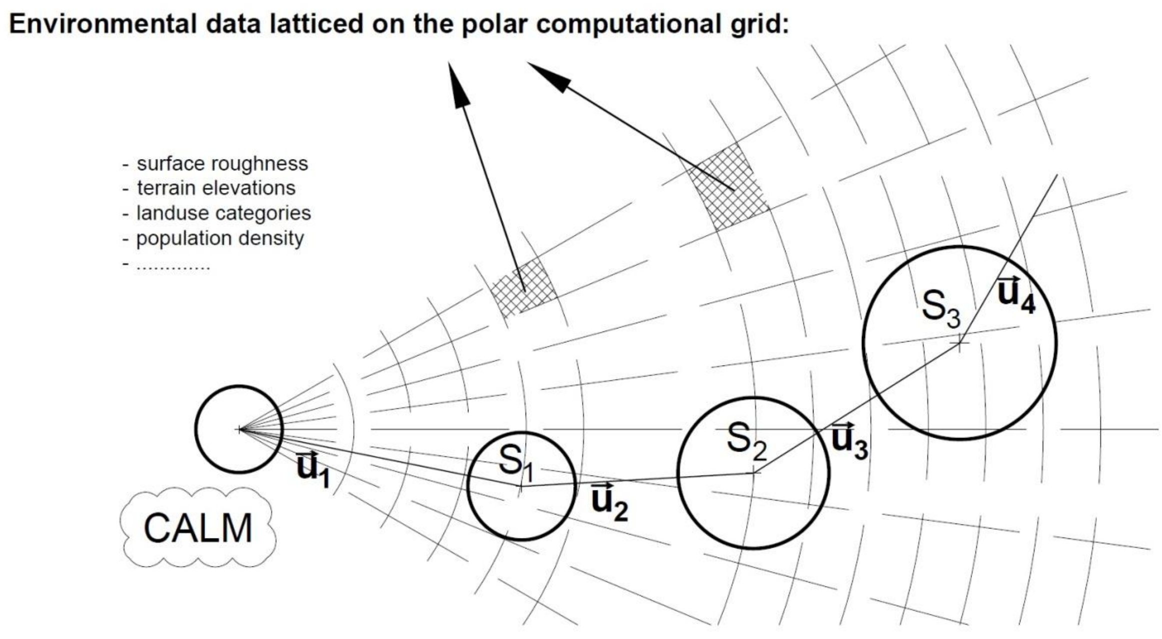

Figure 3. Drift of the CALM results in the next hours of the convective flow.

The Gaussian puff model describing the further convective movement of radioactivity from the calm region is adapted. The initial distribution of concentration entering the first convective stage *p=1* is determined as $C_m^n\left(r, z; T_{END}^{CALM}\right)$. Depletion of the original discharge Q_m^n from its birth at t_m up to T_{END}^{CALM} is expressed as

$$Q_m^n\left(T_{END}^{CALM}\right) = \quad Q_m^n(t_m)\cdot\ f_R^n\left(t_m \rightarrow T_{END}^{CALM}\right)\cdot\ f_F^n\left(t_m \rightarrow T_{END}^{CALM}\right)\cdot\ f_W^n\left(t_m \rightarrow T_{END}^{CALM}\right) \qquad (4.1)$$

This expression belongs to the low-wind conditions formulated in time-representation. For the convective transport, the equivalent expression should be formulated based on the distances passed along the puff trajectory when the type of landuse and orography are incorporated. The parcel of radioactivity is successively drifted at hourly intervals (stages) *p (p=1, ...)* with the velocity values $\vec{u}_p$ and with other parameters of this scenario pertaining to the hourly changes in *p*. The length of the puff centre shift within a particular stage *p* is denoted by l_p, the total length of the puff centre from beginning of the first stage *p=1* to the end of stage *p* is denoted by L_p. The radioactivity dispersion and depletion take place within the convective stage *p*. For the end of the p^{-th} stage of the convective transport the discharge $Q_m^n\left(T_{END}^{CALM}\right)$ is further reduced by the depletion factor F_p^n, which coincides with the puff progress:

$$F_p^n\left(L_p\right) = f_R^n\left(L_p\right)\cdot\ f_F^n\left(L_p\right)\cdot\ f_W^n\left(L_p\right) \qquad (4.2)$$

This accounts for all possible mechanisms of activity removal pertaining to the convective transport of the puff. $L_p = \left(\left|\vec{u}_1\right| + \left|\vec{u}_2\right| + \cdots + \left|\vec{u}_p\right|\right) \times 3600 = \sum_{k=1}^{k=p} l_k$ (in [m]) is a length of the straight-line parts of the puff centre trajectory up to the end of stage *p* relative to the beginning of *p=1*. Dispersion coefficients σ_r and σ_z should be calculated differentially, according to the scheme

$$\sigma\left(L_p\right) = \sigma(T_{END}^{CALM}) + \Delta\sigma\left(\ L_p\ \right) \qquad (4.3)$$

As stated above, the vertical and horizontal dispersion coefficients $\sigma(T_{END}^{CALM})$ are expressed by time-dependent empirical recommendations based on the field measurements under low-wind speed conditions. The downwind concentrations of airborne pollutants during the convective transport are determined on the basis of the coefficients of lateral and vertical dispersions. The key variable is the surface roughness during the puff-surface interaction. Semi-empirical formulae for dispersion $\Delta\sigma\left(\ L_p\ \right)$ either for smooth terrain or, alternatively, for rough terrain of the Central European type can be chosen for convective flow.

The final expression for the activity concentration at the end of the p^{-th} stage of the convective transport has in analogy with (2.2a) the following symbolic form

$$C_{m,p}^n(r,z) = \frac{Q_m^n\left(T_{END}^{CALM}\right)}{(2\pi)^{3/2}\cdot\sigma_r^2\left(L_p\right)} \times \exp\left(-\frac{r^2}{2\cdot\sigma_r^2\left(L_p\right)}\right)\cdot\Psi\left(z, \sigma_z\left(L_p\right), h_{ef,m}\right)\cdot F_p^n\left(L_p\right) \qquad (4.4)$$

where $\Psi\left(z, \sigma_z\left(L_p\right), h_{ef,m}\right) = \frac{1}{\sigma_z\left(L_p\right)}\cdot\left\{\exp\left(-\frac{\left(z-h_{ef,m}\right)^2}{2\cdot\sigma_z^2\left(L_p\right)}\right) + \exp\left(-\frac{\left(z+h_{ef,m}\right)^2}{2\cdot\sigma_z^2\left(L_p\right)}\right)\right\}$

Here *(r, z)* are the coordinates relative to the centre of the puff, $\sigma(L_p)$ is given by (4.3), $F_p^n(L_p)$ is the whole plume radioactivity depletion on the path L_p . A detailed review of relevant parameterizations for modelling of the depletion mechanisms is given in *Sportisse, 2007*. Based on the field measurements, the parameterized models for dry deposition velocities and wet scavenging are compiled.

Quantification of all depletion mechanisms from (4.2) during the convective puff movement is given onwards.

4.1 Depletion of the drifted puff due to radioactive decay

The radioactive decay occurs in the entire puff volume and the corresponding depletion along the path of the particular stage *p* is defined as $\exp\left(-\lambda^n \frac{\mathrm{l_p}}{|\vec{u}_p|}\right)$. In total, the depletion of the puff in its path from *p=1* up to the end of the stage *p* can be expressed as

$$f_R^n(L_p) = \prod_{k=1}^{k=p} \exp\left(-\lambda^n \frac{\mathrm{l_k}}{|\vec{u}_k|}\right) \tag{4.5}$$

where λ^n (s^{-1}) denotes the constant of radioactive decay.

4.2 Depletion of radioactivity in the course of convective transport due to dry deposition (FALLOUT)

The dry deposition generally means the removal of pollutants by sedimentation under gravity, diffusion processes or by turbulent transfer resulting in impacts and interception. The formulation of the radioactivity propagation over the ground is expressed in notation of the source depletion model. The model roughly assumes that the depletion occurs over the entire depth (vertical column) rather than at the surface. The puff's vertical profile is therefore invariant with respect to distance (*Hanna, 1982)*. However, the concentrations of activity along the axis can be somewhat overestimated.

Let us assume the transport in the *p-th* stage according to Fig. 3. Our aim is to derive the term $f_F^n(L_p)$ from Eq. (4.2). The amount of radioactivity in the puff entering stage *p>1* is labelled as $Q_{m,L_{p-1}}^n$ and the corresponding concentration $C_{m,p}^n(r,z)$ is expressed in accordance with Eq. (4.4). For *p=1*, the amount $Q_{m,p}^n$ is given by Eq. (4.1) and the term $C_{m,p}^n(r,z)$ means the particular component $C_{m,i=M-m+1}^n(r,z)$ from Eq. (3.1) or $C_m^n(T_{END}^{CALM}\,; r, z)$. Specifically, let us analyse the fallout during the transport at stage *p* within the interval $l \in < 0\ ;\ l_p >$ when the centre of the puff is moving linearly with velocity $\vec{u}_p$ along the abscisa $S_{p-1}S_p$. For the puff in position *l*, the dry deposition flux over the ground $\dot{\Omega}_{m,p}^n(l\,; z=0)$ [Bq.s^{-1}] from the entire puff is given by

$$\dot{\Omega}_{m,p}^n(l; z=0) = vg_p^n(l)\cdot \int_0^{\infty} C_{m,p}^n(l\,; r, z=0)\cdot 2\pi \cdot r \cdot dr \tag{4.6}$$

Using (4.4), the near-ground activity concentration in the interval $l \in < 0\ ;\ l_p >$ is changing according to

$$C^n_{m,p}(l\,;r,z=0)=\frac{2\cdot Q^n_{m,p}(l)}{(2\pi)^{3/2}\cdot\sigma_r^2(L_{p-1}+l)\cdot\sigma_z(L_{p-1}+l)}\times \tag{4.7}$$

$$\times\exp\left(-\frac{r^2}{2\cdot\sigma_r^2(L_{p-1}+l)}\right)\cdot\exp\left(-\frac{(h_{ef,m})^2}{2\cdot\sigma_z^2(L_{p-1}+l)}\right)$$

Substituting (4.7) into (4.6), the radioactivity deposition flux over the ground from the entire puff equals

$$\dot{\Omega}^n_{m,p}(l;\,z=0)=\;Q^n_{m,p}\,(l)\cdot vg^n_p(l)\cdot\sqrt{\frac{2}{\pi}}\cdot\frac{1}{\sigma_z(L_{p-1}+l)}\cdot\exp\left(-\frac{(h_{ef,m})^2}{2\cdot\sigma_z^2(L_{p-1}+l)}\right) \tag{4.8}$$

After the puff shift $dl{=}u_p\;.\;dt$, the source of radioactivity will be depleted according to $\frac{dQ^n_{m,p}(l)}{dl}=\frac{dQ^n_{m,p}(t)}{u_p\cdot dt}=-\;\dot{\Omega}^n_{m,p}(l;\,z=0)$, and after substitution from (4.8) and smoothing we get

$$\frac{dQ^n_{m,p}(l)}{Q^n_{m,p}(l)}=-\;u_p\cdot vg^n_p(l)\cdot\sqrt{\frac{2}{\pi}}\cdot\frac{1}{\sigma_z(L_{p-1}+l)}\cdot\exp\left(-\frac{(h_{ef,m})^2}{2\cdot\sigma_z^2(L_{p-1}+l)}\right)\cdot dl \tag{4.9}$$

Provided that $Q^n_{m,p}(l=0)=Q^n_{m,L_{p-1}}$, we can write the final expression for the partial fallout depletion of stage p in interval $l\in$<$0;\,l_p$> as

$$\frac{Q^n_{m,p}(l=l_p)}{Q^n_{m,L_{p-1}}}=\;\exp\left\{-u_p\cdot\sqrt{\frac{2}{\pi}}\cdot\int_0^{lp}vg^n_p(l)\cdot\frac{1}{\sigma_z(L_{p-1}+l)}\cdot\exp\left(-\frac{(h_{ef,m})^2}{2\cdot\sigma_z^2(L_{p-1}+l)}\right)\cdot dl\right\} \tag{4.10}$$

Finally, the total fallout depletion in all convective stages *1=1, ... , p* on the path *<0 ; L_p >* is given (in correspondence with (2.8) and (4.2)) as

$$f^n_F(L_p)=Q^n_{m,L_p}\;/\;Q^n_m(T^{CALM}_{END})=$$

$$\prod_{\mathbf{k}=1}^{k=p}\exp\left\{-u_k\cdot\sqrt{\frac{2}{\pi}}\cdot\int_0^{l_k}vg^n_k(l)\cdot\frac{1}{\sigma_z(L_{k-1}+l)}\cdot\exp\left(-\frac{(h_{ef,m})^2}{2\cdot\sigma_z^2(L_{k-1}+l)}\right)\cdot dl\right\} \tag{4.11}$$

The integrals above are solved numerically because of the strong dependency of $vg^n_k(l)$ on the spatial landuse categories of the input environmental gridded data distributed on the fine discrete polar computational network (grid), as indicated in Fig. 3. The identification between relative coordinate *l* and respective absolute landuse gridded coverage on the real terrain is established and put into operation.

4.3 Depletion of radioactivity in the course of the convective transport due to washout by atmospheric precipitation

Similar to Section 2.3, we assume rain of a constant precipitation rate $\upsilon_{m,p}$ (mm/h) during the entire convective stage *p*. The deposition activity rate of nuclide *n* being washed out from the cloud is expressed with the aid of washing (scavenging) coefficient $\Lambda^n_{m,p} = a \cdot (\upsilon_{m,p})^b$ [s^{-1}]. $\upsilon_{m,p}$ is averaged over the entire partial convective stage *p*. Likewise (2.9), the wet deposition flux $\dot{W}^n_{m,p}$ [Bq.s^{-1}] from the entire puff with its centre at *l* is given by

$$\dot{W}^n_{m,p}\left(l\right) = \Lambda^n_{m,p} \cdot \int_0^\infty \left[\int_0^\infty C^n_{m,p}\left(l\,;r,z\right) \cdot dz\right)\right] \cdot 2\pi \cdot r \cdot dr \tag{4.12}$$

The activity concentration $C^n_{m,p}\left(l\,;r,z\right)$ belonging to the puff centre at *l* has the form

$$C^n_{m,p}\left(l\,;r,z\right) = \frac{Q^n_{m,p}\left(l\right)}{\left(2\pi\right)^{3/2} \cdot \sigma^2_r\left(L_{p-1}+l\right)} \times \tag{4.13}$$

$$\times \exp\left(-\frac{r^2}{2\cdot\sigma^2_r\left(L_{p-1}+l\right)}\right) \cdot \Psi\left(z, \sigma^2_z\left(L_{p-1}+l\right), h_{ef,m}\right)$$

The function Ψ is given according to (4.4). The depletion of radioactivity during differential shift $dl = u_p \,.\, dt$ of the puff with its centre at a relative position of *l* is $dQ^n_{m,p}\left(l\right)/dl = 1/u_p \cdot dQ^n_{m,p}\left(l\right)/dt = -\dot{W}^n_{m,p}\left(l\right)$. Substituting (4.13) into (4.12) and proceeding in a way similar to the construction of expression (2.11), the resulting differential equation takes on the form

$$\left.\frac{dQ^n_{m,p}\left(l\right)}{Q^n_{m,p}\left(l\right)}\right|_{wash} = -\Lambda^n_{m,p} \cdot u_p \cdot \sqrt{\frac{2}{\pi}} \cdot \left[\int_{z=0}^{\infty} \Psi\left(z, \sigma^2_z\left(L_{p-1}+l\right), h_{ef,m}\right) \cdot dz\right] \cdot dl \tag{4.14}$$

After integration on $l \in < 0\,;\, l_p >$, we obtain

$$\frac{Q^n_{m,p}\left(L_p\right)}{Q^n_{m,p-1}\left(L_{P-1}\right)} = \tag{4.15}$$

$$= \exp\left\{-\Lambda^n_{m,p} \cdot u_p \cdot \sqrt{\frac{2}{\pi}} \cdot \int_{l=0}^{l=lp}\left[\int_{z=0}^{\infty} \Psi\left(z, \sigma^2_z\left(L_{p-1}+l\right), h_{ef,m}\right) \cdot dz\right] \cdot dl\right\}$$

The following chain holds true

$$\left(Q^n_{m,p} \,/\, Q^n_m\left(T^{CALM}_{END}\right)\right)_{wash} =$$

$$= \left(Q^n_{m,p} \,/\, Q^n_{m,p-1}\right)_{wash} \cdot \left(Q^n_{m,p-1} \,/\, Q^n_{m,p-2}\right)_{wash} \cdot \ldots \cdot \left(Q^n_{m,2} \,/\, Q^n_{m,1}\right)_{wash} \cdot \left(Q^n_{m,1} \,/\, Q^n_m\left(T^{CALM}_{END}\right)\right)_{wash}$$

Finally, the overall washing factor $f^n_W\left(L_p\right)$ defined by (4.2) for the puff movement on all convective stages passing through $<0\,;\, L_p>$ is marked as:

$$f^n_W\left(L_p\right) = Q^n_{m,p} \,/\, Q^n_m\left(T^{CALM}_{END}\right) = \tag{4.16}$$

$$= \prod_{\mathbf{k}=1}^{k=p} \exp\left\{ -\Lambda_{m,k}^{n} \cdot u_k \cdot \sqrt{\frac{2}{\pi}} \cdot \int_{0}^{lk} \left[\int_{z=0}^{\infty} \Psi\left(z, \sigma_z^2\left(L_{k-1}+l\right), h_{ef,m}\right) \cdot dz \right] \cdot dl \right\}$$

For $k=1$ is $L_{k=0} = 0$ and dispersion is further determined with help of expression (4.3).

5 Results

A hypothetical release of radionuclide ^{137}Cs is divided into two stages. In the first two hours, a calm meteorological situation is assumed. The same discharge of Q_m = 1.0 E+07 Bq is released into the motionless ambient every 20 minutes. Following Fig. 1 we have adjusted M=6. Just after the two hours of calm, the wind starts blowing and the convective transport of the radioactivity clew immediately arises. Meteorological data are extracted from stepwise forecast series for a given point of radioactive release, when hourly changes of the wind direction and velocity together with Pasquill category of atmospheric stability are given in Table 3.

Table 3. Hourly changes of meteorology conditions during the convective transport.

Hour	wind speed at 10m height, $m \cdot s^{-1}$	wind direction (°)$^{(*)}$	Pasquill category	precipitation $mm \cdot hour^{-1}$
1	3.0	279	D	0.0
2	4.0	315	D	0.0
3	3.0	346	D	1.0
4	….	….	….	…..

$^{(*)}$ clockwise, from North

The results of several tests displayed on the map background of the Czech nuclear power plant Dukovany are given in Figures 4, 5 and 6. The deposition of radionuclide ^{137}Cs on the ground is indicated for a meteorological situation without rain (Figure 4) against the occurrence of atmospheric precipitation in the third hour of the convective transport (Figure 5).

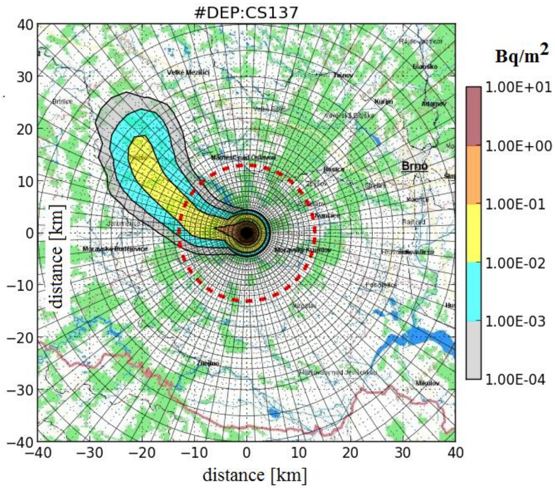

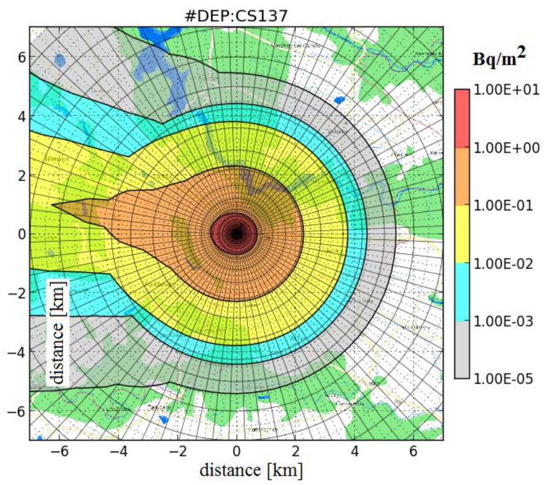

Figure 4. Deposition of radionuclide ^{137}Cs on terrain (sum of 2 hours calm situation plus 3 hours of convective movement). No atmospheric precipitation. Left: Near vicinity up to 40 km from the source of pollution. Right: More detailed image in the original calm region inside the emergency planning zone after the five hours.

Washout of radioactive aerosols due to the processes of rainout and washout are lumped together through the so-called scavenging coefficient mentioned above in Section 2.3 and 4.3. A "fattening" of the washed-out radioactivity on the terrain caused by precipitation in the third hour of convective transport is shown in Figure 5. Its left part detects the occurrence of a small red patch of the higher level of the radioactivity. The right side predicates considerable impact of more intensive atmospheric precipitation when the "hot spot" radioactivity deposition values can increase more than one order of magnitude, even in the distances tens kilometres from the source of pollution.

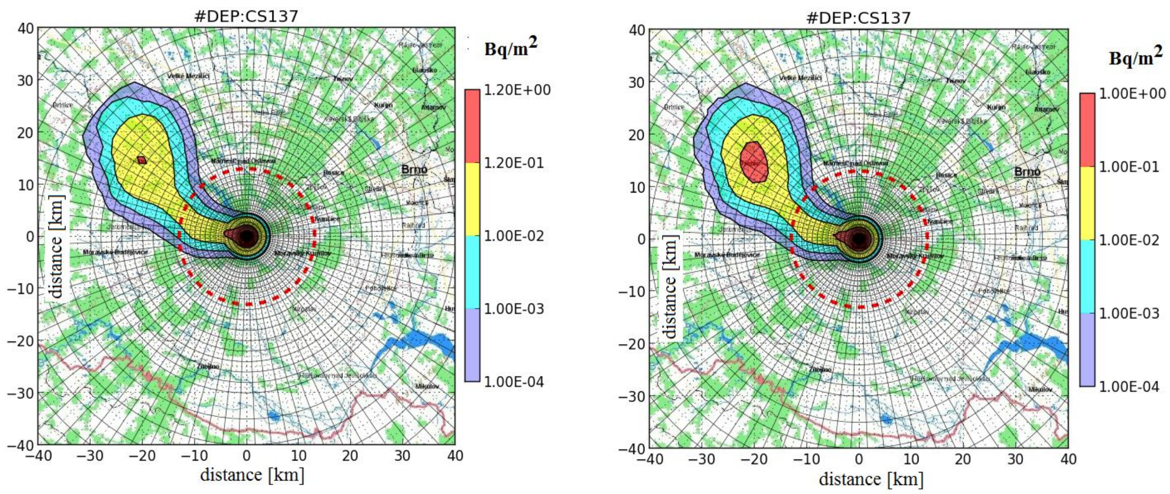

Figure 5. "Hot spots" of deposited radionuclide ^{137}Cs on terrain. Sum of 2 hours calm situation plus 3 hours of the convective movement in the case of atmospheric precipitation in the third hour of the convective transport. Left: Rain with intensity 0.5 mm.h^{-1} . Right: Rain with intensity 1.0 mm.h^{-1} .

The presented scenario incorporates several uncertainties. Important questions arise from the mapping of the gravitational settling values. The effect of this parameter is included in the dry deposition parameterization by a combination of Stokes' law with the Cunningham correction factor for small particles. The importance of the aerosol particle sizes can be inferred from Figure 6. The value vg^n_{grav} = 0.008 m·s^{-1} has been selected for further calculations (see Section 2.2) as an upper guess. The alternative results have been reached with a decreased value vg^n_{grav} = 0.001 m·s^{-1}. For small aerosol sizes (~1.0 μm) we assume this value as a lowest guess. The higher vg^n_{grav} , the higher radioactivity remains permanently deposited in the original calm region, and vice versa. Particularly, a poor deposition from Figure 6 Right implies a higher radioactivity in the cloud entering the surrounding environment in the successive convective phases. Redistribution of radioactivity between the calm and convective regions is apparent.

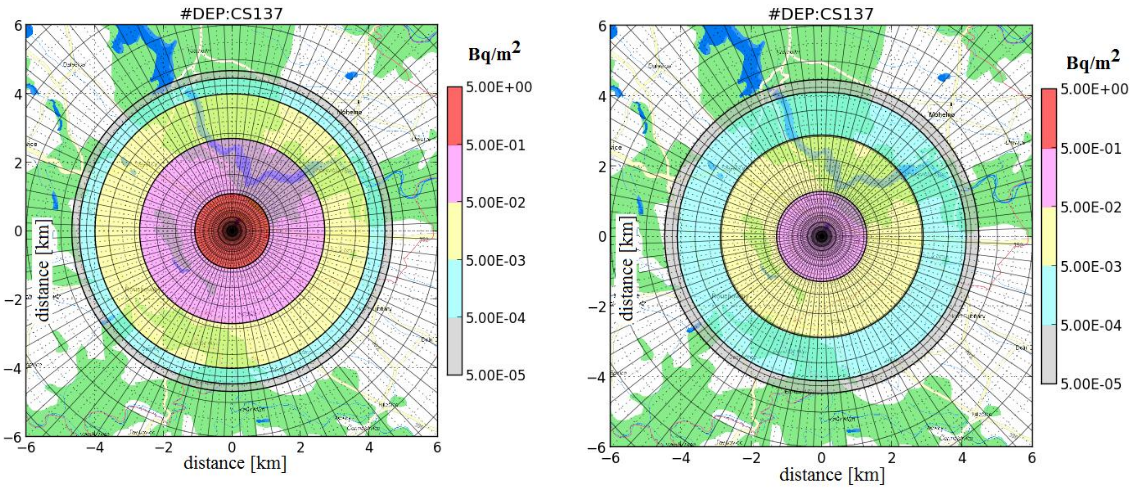

Figure 6. Redistribution of the deposited radioactivity of ^{137}Cs on the ground (deposition in calm region just at the end of the calm situation at the time T_{END}^{CALM}) for different values of the gravitational settling. Left: vg^{n}_{grav} = 0.008 m·s^{-1} , Right: vg^{n}_{grav} = 0.001 m·s^{-1}.

6 CONCLUSIONS

Detailed algorithm for estimating the radiological impact of a hypothetical radiation accident during an atypical calm meteorological situation is presented. Discharges of the radioactivity into the motionless ambient atmosphere can produce an adverse effect of significant radioactivity accumulation near the source of pollution. The instant successive windy conditions replacing the calm leads to the drifting of the “radioactivity reservoir“ and causes dissemination of the harmful substances into the environment. The transport of the aerosol particles is considered in detail, including the activity depletion mechanisms of radioactive decay, dry activity deposition from the cloud and radioactivity washout by potential atmospheric precipitation. Respective equations are formulated for the sophisticated numerical scheme, separately for the calm ambient and the convective movement. Although the probability of a long calm episode is low, its possible consequences can be serious; therefore it is worth examining. The results show a significant increase of radioactivity (especially in combination with rain), which can lead to occurrence of the considerable radioactivity hot spots rather far from the release source. The code can facilitate the estimation of sensitivity of the results with respect to the uncertain values of a certain essential input parameters (e.g. the gravitational settling - see Figure 6). Another important application of the presented algorithm is its capability to simulate a dynamics of the release of contamination on basis of a large number of diverse discrete pulses.

7 REFERENCES

Adriaensen, S., Cosemans, S., Janssen, L. and Mensink, C. (2002) : PC-Puff: A simple trajectory model for local scale applications. *Risk Analysis III, CA Berbia (ED.). ISBN 1-85312-915-1*.

Anfossi, D., Alessandrini, S., Trini Castelli, S., Ferrero, E., Oettl, D. and Degrazia, G., 2006. Tracer dispersion simulation in low wind speed conditions with a new 2D Langevin equation system. *Atmospheric Environment 40 (2006) 7234–7245.*

Carruthers, D. J., Weng, W. S., Hunt, J.R.C., Holroyd, R.J., McHugh, C.A. and Dyster, S.J. (2003) : PLUME/PUFF Spread and Mean Concentration - Module Specifications. *ADMS3 paper P10/01S/03, P12/01S/03*.

Hanna, R. S., Briggs, G. A. and Hosker (Jr.), R.P. (1982): Handbook on Atmospheric Diffusion. *DOE/TIC-11 223, (DE82002045).*

HARP (2010-2019): Environmental SW package HARP (**HA**zardous **R**adioactivity **P**ropagation). URL: *https://havarrp.utia.cas.cz/harp*

Horst, T.W. (1977): A Surface Depletion Model for Deposition from a Gaussian Plume. Atmospheric Environment Vol. 11, pp. 41-46.

Hyojoon, J., Misun, P., Wontae H., Enuhan, K., and Moonhee, H. (2013): The effect of calm conditions and wind intervals in low wind speed on atmospheric dispersion factors. *Annals of Nuclear Energy 55 (2013) pp. 230-237.*

EPA, 2004. AERMOD: Description of Model Formulation. U.S. Environmental Protection Agency, Research Triangle Park, NC (Report EPA-454/R-03-004).

Jeffrey, C.A., Paine, R.J. , Hanna, S. (2013): AERMOD low wind speed issues: Review of new model release. *Memorandum of American Meteorological Society (AMS) / US Environmental Protection Agency (EPA).*

Jones, J. A. (1996): Atmospheric Dispersion at Low Wind Speed. *Liaison Comm. Annual Report, 1996-1997, ANNEX A, NRPB-R292.*

Lines, I.G. and Deaves, D.M. (1997) : Atmospheric Dispersion at Low Wind Speed. *Liaison Comm. Annual Rep., 1996-1997, NRPB-R302.*

McGuire, S.A., Ramsdell, J.V. and Athey ,G.F. (2007) : RASCAL 3.0.5: Description of Models and Methods. *NUREG – 1887*.

Okamoto, S., Onishi, H., and Yamada T. (1999): A Model for Simulating Atmospheric Dispersion in a Low-Wind Condition. *In: Proceedings of 6HARMO conf., Rouen.*

Pandey, G. and Sharan,M. 2019. Accountability of wind variability in AERMOD for computing concentrations in low wind conditions. *Atmospheric Environment 202 (2019) 105–116.*

Pecha, P., Pechova, E. (2004): Risk Assessment of Radionuclide Releases during Extreme Harmonisation within Atmospheric Dispersion Modelling for Regulatory Purposes, p. 320-324, (Garmisch-Partenkirchen, DE, 01.06.2004-04.06.2004). URL: *https://havarrp.utia.cas.cz/harp/reporty_PDF/poster_LowWind_Harmo9.pdf*

Pöllänen, R., Toivonen H., Lahtine, J., and Ilander, T. (1995): Transport of Large Particles Released in a Nuclear Accident. *STUK-A125, OCTOBER 1995.*

Qian, W. and Venkatram, A. (2011): Performance of steady-state dispersion models under low wind-speed conditions. *Boundary-Layer Meteorol. 138, 478–491.*

Rakesh, P.T., Venkatesan, R., Srinivas, C.V., Baskaran, R. and Venkatraman, B. (2019): Performance evaluation of modified Gaussian and Lagrangian models under low wind speed: A case study. *Annals of Nuclear Energy 133 (2019) 562–567.*

Sportisse, B. (2007): A review of parameterization for modelling dry deposition and scavenging of radionuclides. Atmospheric Environment 41 (2007), pp. 2683-2698.

Tsuda, A., Henry, F. S. and Butler, J.P. (2013): Particle transport and deposition: basic physics of particle kinetics. *Compr. Physiol. 3(4), pp. 1437-1471.*

Zannetti, P. (1990): Air Pollution Modeling. Theories, Computational Methods and Available Software. ISBN 1 – 85312-100-2.

WS Atkins Consultants Ltd (1997) : The Implications of Dispersion in Low Wind Speed Conditions for Qualified Risk Assess. *CRR 133/1997, ISBN 0 7176 1359 3.*